

An Optimal Numerical Model for Nonlinear Behavior of Reinforced Concrete Frames

D. Kovačević^{1*}, I. Matijević², A. Rašeta³

Civil Engineering Department, Faculty of Technical Sciences, University of Novi Sad
Trg Dositeja Obradovića 6, 21000 Novi Sad, Serbia

^{1*} dusan@uns.ns.ac.yu

² iv.matijevic@yahoo.com

³ araseta@uns.ns.ac.yu

*Corresponding author

Abstract

This paper is a review of a possibility for numerical modeling of in-plane reinforced concrete (RC) frames loaded by various loadings. Research scope is limited only to beam/column frame structures without wall/plate structural elements. The objective of this research is a formulation of an enough sophisticated and, for civil engineering design purposes - "optimal" i.e. reasonably convenient numerical model.

Structural discretization and mathematical approximations are based on the finite element method (FEM) concept. For modeling concrete and steel nonlinear behavior uniaxial constitutive rules for these materials are used. The steel-concrete bond relation is modeled indirectly - by tension stiffening effect. As opposed to standard one-dimensional "1D" beam FE models, that includes only the concrete and reinforcement behavior modeling, the suggested two-dimensional "2D" beam FE model includes the interaction of shear and flexural forces.

The proposed model is based on "2D" beam FE with capabilities of sophisticated models. The introduced numerical concept for simulation of structural behavior of RC frames loaded by various loads (from simple static to complex cyclic) is formulated as a compromise solution. The compromise is made between accuracy, as an essential parameter, and, on the other hand, simplicity, as everyday design practice task. The objective of presented research was to find the "middle way" (synchronized accuracy and numerical efficiency) in nonlinear analyses of the described RC frame structures.

Keywords: FEM, Numerical Modeling, Nonlinear Analysis, RC Frames

1. Introduction

Structural modeling is the process of creation of idealized and simplified representation of structural behavior and it is an essential step in structural analysis and design. Errors and inadequacies in modeling may cause serious design defects and difficulties. Numerical modeling is a mathematical realization of selected structural modeling concept.

Due to numerical efficiency and simple software implementation, the FEM has become a fundamental method of structural analysis and numerical modeling of RC structural behavior. Basic classification of numerical models for RCs is presented by a scheme in Fig. 1.

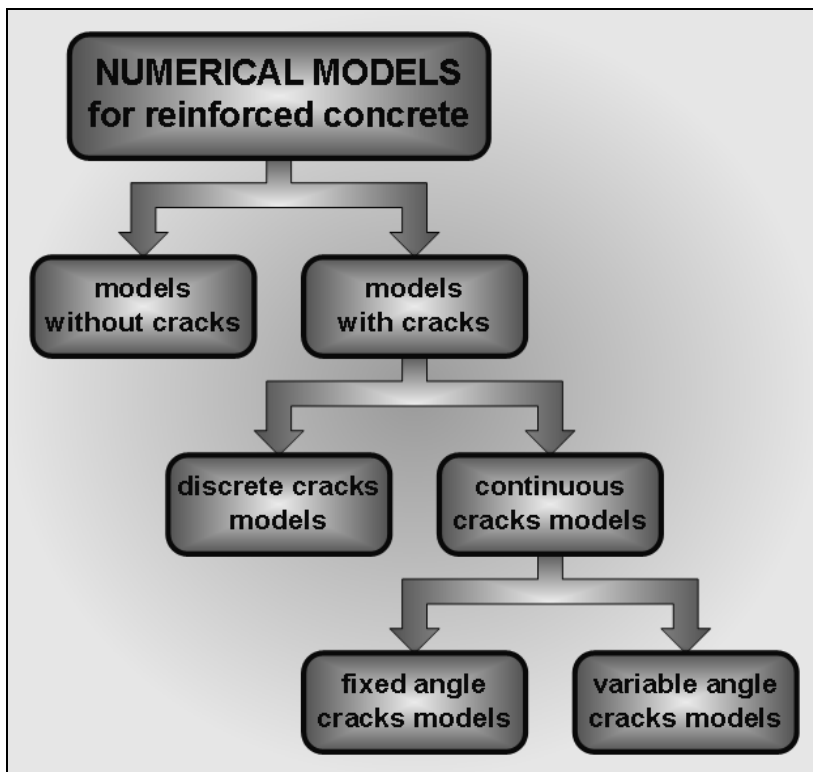


Fig. 1. Numerical models for reinforced concrete.

The following model groups can summarize another classification of RC models.

3D (3-dimensional solid) FE models enable the highest quality of approximation, but model complexity and difficulties in their application (first of all, computation costs) make structural analysis of real buildings quite hard. Therefore, 3D FE models can be adopted as benchmark-test models, for verification of simpler (2D or 1D) models.

2D (membrane, plate, shell) FE models are frequently used in numerical analysis of RC beams, especially for the research of so-called "local effects" ("aggregate interlock", "dowel action", etc.). Basic advantage in comparison to models with beam FE lies in a possibility of modeling the shear stresses influence to RC elements mechanical response.

1D (beam) FE models are the simplest and make nonlinear analysis possible in everyday engineering practice, and not only in the phase of preliminary design. Moreover, application of the 2D beam FE provides results that confirm adequate quality of approximation, shown even in initial research of Blaauwendraad et al. (1983) and Scordelis (1984).

A simple example demonstrates the basic differences between these three model groups, Fig. 2. Similar results were obtained in both linear and nonlinear analysis. Computer resources which are needed for the analysis of these examples are different not only in quantitative but in qualitative manner.

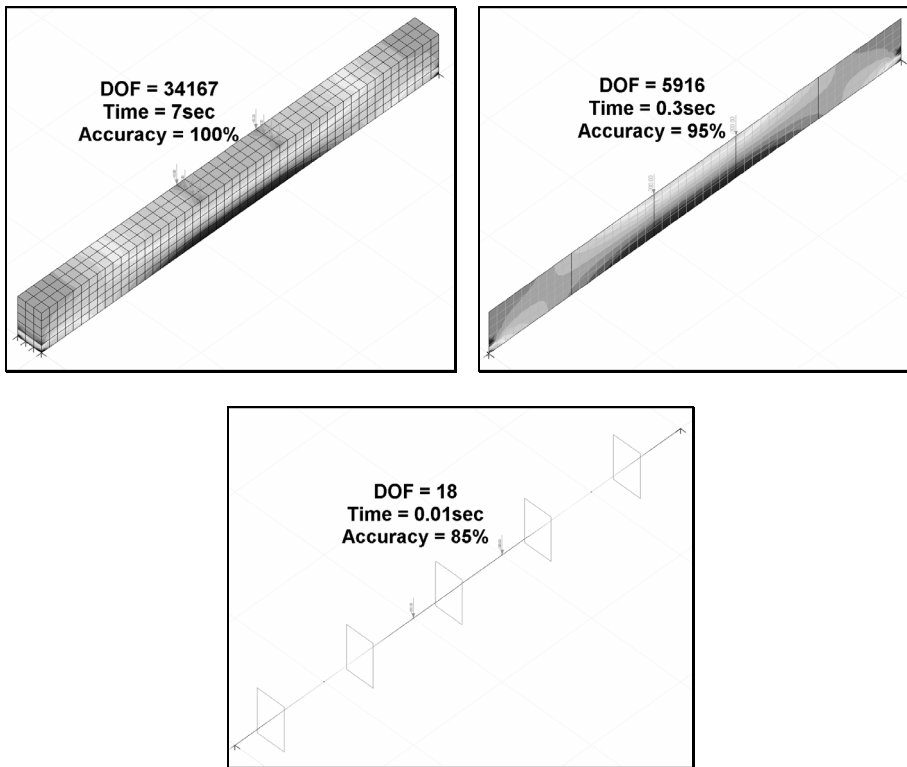


Fig. 2. Different numerical models for the simple supported beam - comparison of number of degrees of freedom (DOF), accuracy with respect to the 3D solution (as the baseline solution), and computational times.

Particularly, the main goal of structural modeling is to adopt an "optimal" model - a compromise between complexity and quality of approximation. Such optimal model should provide a sufficient reliability in prediction of the "real" structural behavior (quality of approximation), with complexity that corresponds to the given computation capabilities.

Although methods of numerical analysis, computer technology, system and applicative software are continuously developing, one always searches to find the simplest models. It is necessary to emphasize that numerical model quality should be determined by the overall structural behavior modeling quality, not only according to "local" effects modeling ability.

In next section, some details about model proposal are presented: basic assumptions, fundamental relations and derived equations, FEM representation, material behavior modeling concept, and some numerical aspects. Finally, as an illustration of the proposed model, several numerical examples are given.

2. Model with 2D beam FE - basic assumptions, geometry and coordinates

Beam finite elements may be classified into two basic groups:

1D beam FE - the shear deformations are neglected (Bernoulli-Navier's beam theory), and

2D beam FE - influence of the shear is taken into account (Timoshenko's beam theory).

A criterion for determination of model dimensionality is the number of parameters that define displacement field of the beam FE. In the case of 1D beam FE, the rotation of the cross-section is determined via derivatives of displacement (deflection), while in the case of the 2D beam FE the rotation and the deflection parameters are independent.

The type of discretization could also define the dimensionality of a model. In a nonlinear analysis and application of a beam FE, discretization is usually performed both along the length of the structural element and the height of its cross-section. This circumstance indicates the physical/geometrical two-dimensionality of the problem. All further considerations will be based upon this two-dimensional "2D" beam FE.

In the formulation of the model with two-dimensional beam FE the assumptions are as follows:

Straight, plane, two-joint beam FE approximates a RC element (beam, column). Two displacements and one rotation per joint are the degrees of freedom (DOF), with the corresponding cross-section forces, Fig 3.

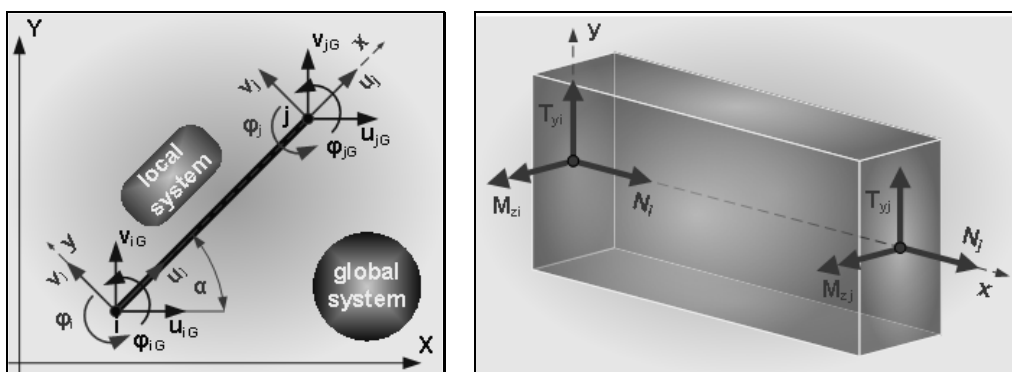


Fig. 3. DOFs and cross-section forces of a beam FE.

A third degree L'Hermite polynomials are adopted for the interpolation of beam lateral displacements and first degree polynomials are adopted for approximation of beam longitudinal displacements. It is conventional and a wide-spread approach.

External loading is applied at the beam FE joints, regardless to real load configuration.

Beam FE cross-section is divided into certain number of finite thickness concrete and steel layers (with area A_i and tangent modulus E_i), Fig. 4, whose behaviors under the loading are modeled by corresponding uniaxial constitutive laws. Selection of number of layers and their influence on the model quality are discussed in Section 8.

The uniform cracks distribution (so-called "smeared cracks approach") is adopted in zones where the concrete tension strength is reached (see Fig. 5).

Linear strain distribution is adopted along the height of the cross-section, because of negligible shear influence in the total deformation field for the common beam. Additionally, the so-called "shear locking" effect (overestimated participation of shear deformation in the total deformation energy) is avoided. It has been proved that a model with unreal high stiffness is obtained, if 2D beam FE with rotation field independent from displacement field is employed. This effect is particularly evident in elements with high length/height ratio and elements characterized with lower level of interpolation (beam with two joints, for example). In contrast

to shear in a strict sense, axial and shear stresses, interaction causes inclined cracks appearance which must be included in model; details are discussed later in Section 7.

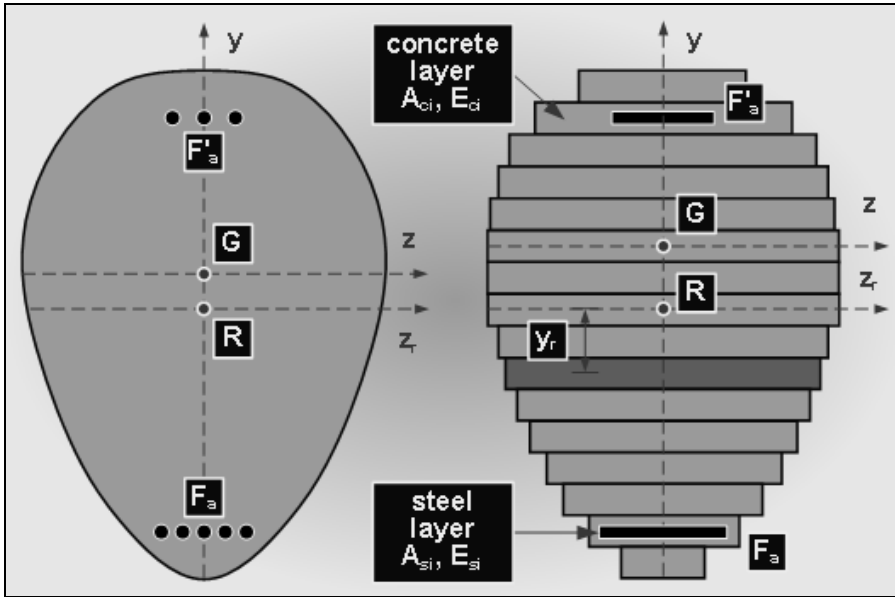


Fig. 4. Layer discretization of a beam FE cross-section.

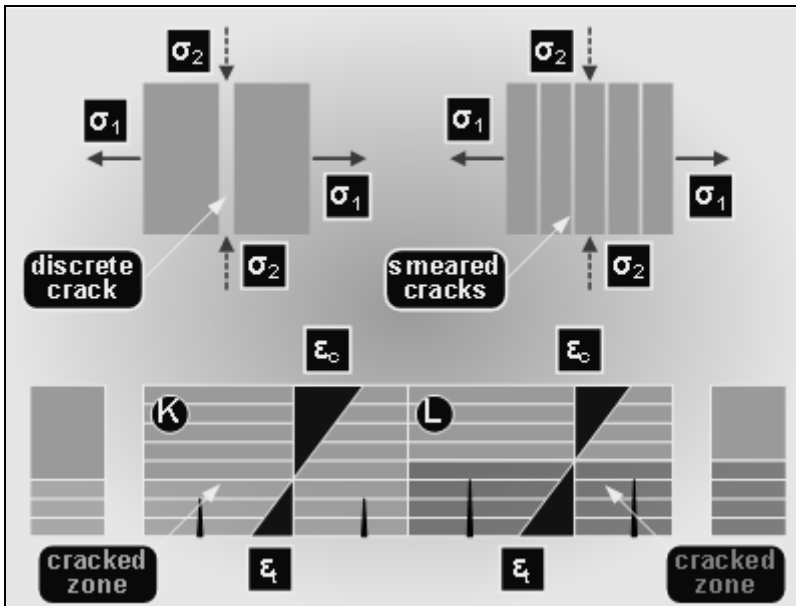


Fig. 5. Continuous, i.e. "smeared" cracks approach.

Concrete-reinforcement interaction (bond) is modeled implicitly by a so-called "tension stiffening effect" (see Fig. 6). Tension stiffening will be included by constitutive law for concrete in tension, as described in Section 6.

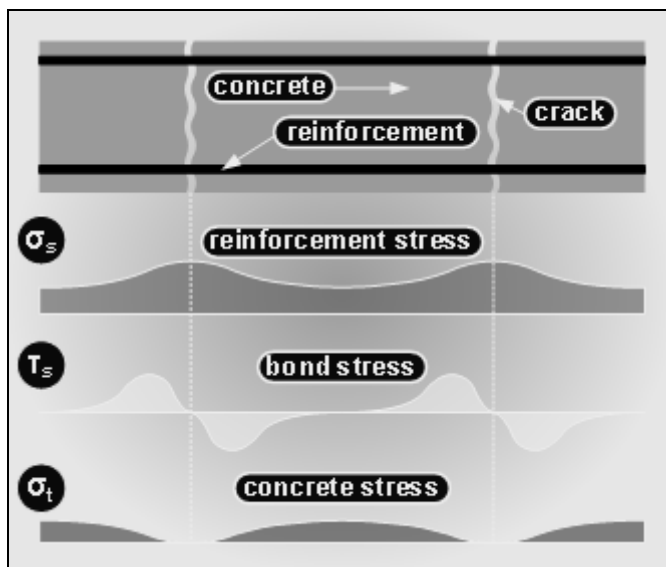


Fig. 6. Tension stiffening as a consequence of concrete-reinforcement bond stress distribution.

3. Constitutive relations and incremental equilibrium equation of the beam FE

In nonlinear analysis (large displacements and material nonlinearity), incremental form of solution is usually adopted, where the increments of displacements are the basic unknowns. In formulating the incremental relations for the beam FE, we start from the expression for the strains and displacements:

$$\varepsilon_x = \frac{du(x)}{dx} + \frac{1}{2} \cdot \left(\frac{du(x)}{dx} \right)^2 + \frac{1}{2} \cdot \left(\frac{dv(x)}{dx} \right)^2 \quad (1)$$

where u and v are the axial and lateral displacements. For the plane beam, the second term can be neglected because of its small contribution to overall strain ε_x . Eq. (1) now obtains the form:

$$\varepsilon_x = \varepsilon_{xL} + \varepsilon_{xN} = \frac{du(x)}{dx} + \frac{1}{2} \left(\frac{dv(x)}{dx} \right)^2 \quad (2)$$

The first and second term in this equation represents the linear and nonlinear parts of the total strain ε_x . The linear term is the function of coordinates of each point $P(x_p, y_p)$ of the beam FE. According to the bending theory we have that:

$$\varepsilon_{xL}(x, y) = \frac{du(x)}{dx} = \frac{du_s(x)}{dx} - y \frac{d^2v(x)}{dx^2} \quad (3)$$

The functions $u_s(x)$ and $v(x)$ define the longitudinal and transversal components of displacements. Based on the expressions (2) and (3), the equation that defines the total strain in an arbitrary beam's point is obtained as:

$$\varepsilon_x(x, y) = \frac{du_s(x)}{dx} - y \frac{d^2v(x)}{dx^2} + \frac{1}{2} \left(\frac{dv(x)}{dx} \right)^2 \quad (4)$$

A third degree polynomial as the interpolation function ensures the fulfillment of a compatibility conditions between beam FE joints (C^0 continuity of the function and C^1 continuity of first derivative). Functions $u_s(x)$ and $v(x)$, expressed by interpolation polynomials and the vector of FE joint displacements \mathbf{u} , are:

$$\mathbf{u}_s(x) = [N_1 \ 0 \ 0 \ N_4 \ 0 \ 0] \mathbf{u} \quad (5)$$

$$\mathbf{v}(x) = [0 \ N_2 \ N_3 \ 0 \ N_5 \ N_6] \mathbf{u} \quad (6)$$

where N_1 and N_4 are linear interpolation functions; N_2, N_3, N_5 and N_6 are the third degree L'Hermite's polynomial interpolation functions; and $\mathbf{u}^T = \{u_i, v_i, \varphi_i, u_j, v_j, \varphi_j\}$ is the nodal displacement vector.

The first and second derivatives of the displacements are:

$$\frac{du_s(x)}{dx} = \left[\frac{dN_1}{dx} \ 0 \ 0 \ \frac{dN_4}{dx} \ 0 \ 0 \right] \mathbf{u} = \mathbf{G}_s \mathbf{u} \quad (7)$$

$$\frac{dv(x)}{dx} = \left[0 \ \frac{dN_2}{dx} \ \frac{dN_3}{dx} \ 0 \ \frac{dN_5}{dx} \ \frac{dN_6}{dx} \right] \mathbf{u} = \mathbf{G}_B \mathbf{u} \quad (8)$$

$$\frac{d^2v(x)}{dx^2} = \left[0 \ \frac{d^2N_2}{dx^2} \ \frac{d^2N_3}{dx^2} \ 0 \ \frac{d^2N_5}{dx^2} \ \frac{d^2N_6}{dx^2} \right] \mathbf{u} = \mathbf{B}_B \mathbf{u} \quad (9)$$

The strain follows from these expressions:

$$\varepsilon_x(x, y) = \mathbf{G}_s \mathbf{u} - y \mathbf{B}_B \mathbf{u} + \frac{1}{2} \mathbf{u}^T \mathbf{G}_B^T \mathbf{G}_B \mathbf{u} \quad (10)$$

or

$$\varepsilon_x(x, y) = \mathbf{B} \mathbf{u} + \frac{1}{2} \mathbf{u}^T \mathbf{G}^T \mathbf{G} \mathbf{u} \quad (11)$$

where

$$\mathbf{B} = \mathbf{G}_s - y \mathbf{B}_B \quad \text{and} \quad \mathbf{G} \equiv \mathbf{G}_B \quad (12)$$

Here, the vectors \mathbf{G} and \mathbf{B} correspond to large and small displacements, respectively.

Equilibrium equations in the incremental form can be obtained within the so-called "Lagrange formulation", in terms of the displacement increments as the unknowns. The beam FE state can be analyzed by using three reference configurations: "START", "CURRENT" and "NEXT" in Fig. 7, representing the initial, configuration at start of load step, and configuration at end of load step.

The incremental variant of the Eq. (11), for the current configuration, is:

$$\Delta \varepsilon_x(x, y) = \mathbf{B} \Delta \mathbf{u} + \frac{1}{2} \Delta \mathbf{u}^T \mathbf{G}^T \mathbf{G} \Delta \mathbf{u} \quad (13)$$

Well-known equilibrium condition in tangent form is:

$$d\mathbf{F} = \int_V \mathbf{B}^T E_t \mathbf{B} dV d\mathbf{u} + \int_V \mathbf{G}^T \sigma \mathbf{G} dV d\mathbf{u} \quad (14)$$

or

$$d\mathbf{F} = \mathbf{k}_L d\mathbf{u} + \mathbf{k}_{NL} d\mathbf{u} \quad (15)$$

or

$$d\mathbf{F} = \mathbf{k}_t d\mathbf{u} \quad (16)$$

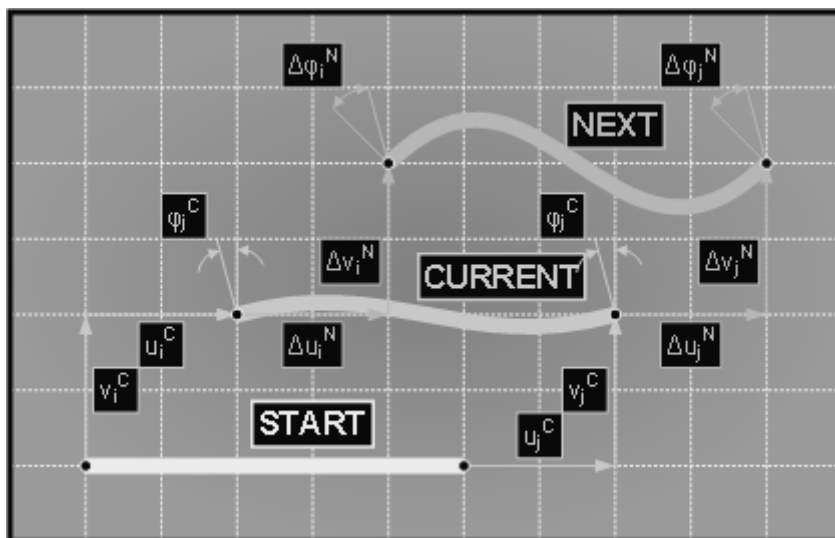


Fig. 7. "START", "CURRENT" and "NEXT" incremental configuration.

where $k_t = \mathbf{k}_L + \mathbf{k}_{NL} = \int_V \mathbf{B}^T E_t \mathbf{B} dV + \int_V \mathbf{G}^T \sigma \mathbf{G} dV$ is tangent stiffness matrix (\mathbf{k}_L and \mathbf{k}_{NL} are the linear and geometrically nonlinear stiffness matrices) and E_t is tangent modulus; and $d\mathbf{F}$ is the increment of external nodal loads (forces and moments).

Equation (15) represents the equilibrium equation of the beam finite element in the local coordination system, in a tangent form. Effects of material nonlinearity are modeled by using elastic-plastic constitutive law which provides the tangent modulus E_t . Effects of geometrical nonlinearity (large displacements and small strains) are modeled by geometrical stiffness matrix \mathbf{k}_{NL} . Errors in modeling large rotations are reduced indirectly, by discretization of beams - increasing number of FEs.

4. Tangent stiffness matrix of 2D beam FE

Coefficients of matrices are determined by using Eq. (13). If the relation $\mathbf{B} = \mathbf{G}_S y \mathbf{B}_B$ is included in the first term of this equation, it is obtained:

$$\mathbf{B} = \left[\frac{dN_1}{dx} \quad -y \frac{d^2 N_2}{dx^2} \quad -y \frac{d^2 N_3}{dx^2} \quad \frac{dN_4}{dx} \quad -y \frac{d^2 N_5}{dx^2} \quad -y \frac{d^2 N_6}{dx^2} \right] \quad (17)$$

If the average value is adopted for the elasticity modulus along the overall length of the element in one layer, the first term in Equation (13) can be written in the form:

$$\mathbf{k}_L = \int_A E_t dA \int_L \mathbf{B}^T \mathbf{B} dx \quad (18)$$

For a constant E_t over the cross-sectional segments and along the element length L , integration along the FE length can be performed analytically, thus obtaining the beam FE stiffness matrix:

$$\mathbf{k}_L = \begin{bmatrix} \frac{EA}{L} & 0 & \frac{ES}{L} & -\frac{EA}{L} & 0 & -\frac{ES}{L} \\ & \frac{12EI}{L^3} & \frac{6EI}{L^2} & 0 & -\frac{12EI}{L^3} & -\frac{6EI}{L^2} \\ & & \frac{4EI}{L} & -\frac{ES}{L} & -\frac{6EI}{L^2} & \frac{2EI}{L} \\ & & & \frac{EA}{L} & 0 & \frac{ES}{L} \\ & & & & \frac{12EI}{L^3} & -\frac{6EI}{L^2} \\ \text{symm.} & & & & & \frac{4EI}{L} \end{bmatrix} \quad (19)$$

$$\text{where} \quad EA = \sum_{i=1}^n E_i A_i \quad ES = \sum_{i=1}^n y_i E_i A_i \quad EI = \sum_{i=1}^n y_i^2 E_i A_i \quad (20)$$

Here, summation is over the cross-sectional layers; S is a cross-section moment of area related to referent axis, and I is the second moment of the cross-sectional area. The term S introduces the cross-section centroid change due to change of stiffness along the cross-section height.

The geometrical stiffness matrix \mathbf{k}_{NL} is obtained using Eq. (8) and the second term of the Eq. (13):

$$\mathbf{k}_{NL} = \int_A \sigma dA \int_L \mathbf{G}^T \mathbf{G} dx = P \int_L \mathbf{G}^T \mathbf{G} dx \quad (21)$$

where P is axial force of the beam. This matrix is:

$$\mathbf{k}_{NL} = P \begin{bmatrix} 0 & 0 & 0 & 0 & 0 & 0 \\ & \frac{6}{5L} & \frac{1}{10} & 0 & -\frac{6}{5L} & \frac{1}{10} \\ & & \frac{2L}{15} & 0 & -\frac{1}{10} & -\frac{L}{30} \\ & & & 0 & 0 & 0 \\ & & & & \frac{6}{5L} & \frac{1}{10} \\ \text{symm.} & & & & & \frac{2L}{15} \end{bmatrix} \quad (22)$$

Equations (19) and (22) define matrices in a local coordinate system. Matrices in a global coordinate system are obtained by application of the transformation:

$$\mathbf{k}_G = \mathbf{T}^T \mathbf{k}_l \mathbf{T} \quad (23)$$

where \mathbf{k}_{iG} is the tangent stiffness matrix in a global coordinate system, and \mathbf{T} is the transformation matrix. For the plane beam, the transformation matrix \mathbf{T} is:

$$\mathbf{T} = \begin{bmatrix} \cos \alpha_c & \sin \alpha_c & 0 & 0 & 0 & 0 \\ -\sin \alpha_c & \cos \alpha_c & 0 & 0 & 0 & 0 \\ 0 & 0 & 1 & 0 & 0 & 0 \\ 0 & 0 & 0 & \cos \alpha_c & \sin \alpha_c & 0 \\ 0 & 0 & 0 & -\sin \alpha_c & \cos \alpha_c & 0 \\ 0 & 0 & 0 & 0 & 0 & 1 \end{bmatrix} \quad (24)$$

where α_c is the angle between local x -axis and global X -axis for a "C" configuration.

The tangent stiffness matrix of the system \mathbf{k}_t is obtained by superposition of the corresponding matrices of FEs, according to the system nodes link, hence we have:

$$\mathbf{k}_t = \sum_{i=1}^n \mathbf{Z}_i^T \mathbf{T}_i^T \mathbf{k}_{t_i} \mathbf{T}_i \mathbf{Z}_i \quad (25)$$

where \mathbf{Z}_i matrices contain zero and unit rows, for non-common and common nodes of the finite elements, respectively.

5. Cross-section forces and FE nodal forces of the structure

Incremental stresses in a beam FE can be obtained from the Eq. (12), as:

$$\Delta \sigma_x(x, y) = E_t \Delta \varepsilon_x(x, y) = E_t \left(\mathbf{B} \Delta \mathbf{u} + \frac{1}{2} \Delta \mathbf{u}^T \mathbf{G}^T \mathbf{G} \Delta \mathbf{u} \right) \quad (26)$$

Forces at joints for each FE of the system (internal structural forces) are obtained from the relations:

$$\mathbf{F}^{\text{int}} = \int_V \mathbf{B}^T \sigma_i dV \quad (27)$$

or, in component form,

$$F_i^{\text{int}} = \int_V B_i \sigma dV = L \int_0^1 B_i ds \int_A \sigma dA \quad (28)$$

The normal stress is a function $\sigma(s, y)$ which, in general case, is specific for each layer of the cross-section and for each beam segment. The forces \mathbf{F}^{int} are obtained by numerical integration, according to the following general expression:

$$F_i^{\text{int}} = \sum_{g=1}^m B_i(s_g) \left(\sum_{l=1}^n -y_l \sigma(l, g) A_l \right) w_g \quad (29)$$

where m is the number of integration points, n is number of layers (l is the layer number) in a cross-section, s_g is the integration point coordinate, and w_g is the weighting coefficient of numerical integration.

Computation of the FE internal nodal forces continues during equilibrium iterations until the convergence is reached, when the internal forces for the current load step are equal to the external loads (within a selected numerical tolerance).

6. Constitutive laws

For modeling of concrete and steel behavior under load, it is necessary to define constitutive laws for both materials. The following combination of constitutive models has been chosen for a concrete structure under cyclic loading (loading, unloading, and reloading), Fig 8:

Hongstad's model for concrete in compression with unloading/reloading option, modified according to the influence of the transversal reinforcement (stirrups),

CEB-FIP model for concrete in tension with unloading/reloading option and with shape which implicitly comprise the tension stiffening, and bilinear model for steel with hardening.

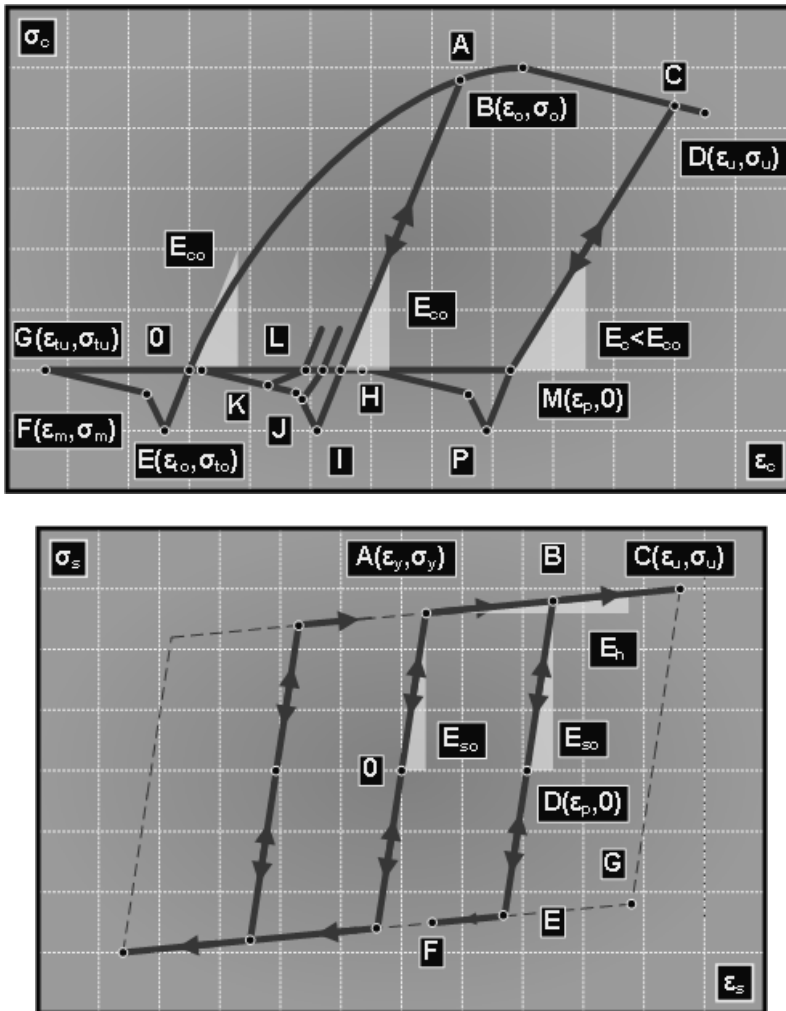


Fig. 8. Adopted constitutive laws for concrete (top figure) and steel (bottom figure) for cyclic loading.

The assumptions are:

plastic creep (yield) of concrete in zone of compression when strain reaches the value ε_o , which corresponds to the stress $\sigma_o = 0.85 \cdot f_c$ (f_c strength of concrete under compression),

failure state in compression zone occurs when the strain reaches a value of limit strain ε_u ,

appearance of cracks in concrete occurs when the strain in tensile zone reaches the value ε_{to} which corresponds to the tensile strength σ_{to} , and

after the appearance of cracks the concrete in that zone cannot carry tensile stresses; but it can carry compression stresses, after the cracks closing during unloading.

Parameters that determine the model are:

initial elasticity modulus of concrete for compression and tension,

compression strength and corresponding strain,

tensile strength and corresponding strain,

limit strain for cracked concrete,

"transition" and limit strain for tensile concrete, and

stirrups distance and area of transversal reinforcement.

In the diagram of adopted constitutive model, the following phases are possible (Fig. 8):

state of compression (segment of the curve 0-A-B),

state of plastic creep (segment of the curve B-C-D),

state of concrete crushing (behind the point D),

state of unloading/reloading, if strains did not reach the value ε_o (line A-H-I),

state of unloading/reloading, if strains have reached the value $\varepsilon_{co} \leq \varepsilon_o$ (segment C-M-N),

tensile state, if strains have not reached the value ε_{to} (straight line O-E),

tensile state, if strains are $\varepsilon_{to} \leq \varepsilon_t \leq \varepsilon_{tm}$ (straight line E-F),

tensile state, if strains are $\varepsilon_{tm} \leq \varepsilon_t \leq \varepsilon_{tu}$ (straight line F-G) and

opening/closing of cracks (horizontal line from the point G).

Modification of Hognestad's model, due to influence of a transversal reinforcement, as described in CEB Bulletin d'information No 210 (1991), has the form:

$$\sigma_c = \sigma_o \alpha \left(2 - \frac{\alpha}{k} \right) \quad \text{for } \varepsilon_o \geq \varepsilon_c \geq 0 \quad (30)$$

$$\sigma_c = k \sigma_o [1 - z(\varepsilon_c - \varepsilon_o)] \quad \text{for } \varepsilon_u \geq \varepsilon_c \geq \varepsilon_o \quad (31)$$

$$k = 1 + r_t \frac{\sigma_y}{\sigma_o} \quad (32)$$

$$z = \frac{0.5}{T_1 + T_2 - 0.002 k} \quad (33)$$

$$T_1 = \frac{3 + 0.2844 f_c}{14.22 f_c - 1000} \quad (34)$$

$$T_2 = 0.75 r_t \sqrt{\frac{b_c}{s_t}} \quad (35)$$

where: σ_y is the stress in reinforcement at yield limit, r_t is ratio between volume of transversal reinforcement (one stirrup) and concrete core comprised of transversal reinforcement (between two neighboring stirrups); b_c is the width of concrete core comprised of stirrups; and s_t is the stirrups distance.

The limit strain of concrete with stirrups is $\varepsilon_{uc} = 0.8/z + \varepsilon_{0k}$. It is taken that $z=75$ for concrete without stirrups. This modification, as opposed to many recommendations, enables modeling the behavior of reinforced concrete elements in cases when a limit-bearing capacity (dynamic and seismic loading) is reached.

It is taken that the residual strain ε_r in tension zone is a function of strain which is reached before start of unloading:

$$\varepsilon_r = \alpha (\varepsilon_t - \varepsilon_{to}) \quad 0 \leq \alpha \leq 1 \quad (36)$$

By adoption $\alpha=0$ it is assumed that in tensile zone there are no residual strains, which does not reflect the reality. On the other hand, it was found that by selection $\alpha \geq 0.5$, relatively large residual strain occurs, and therefore we propose that the value of this coefficient be $\alpha=0.2\sim 0.3$. By varying the coefficient α , the effects of earlier appearance of compression can be modeled in a zone which before unloading was in tension. This state represents a consequence of displacement of parts of the aggregate and cement mortar in zones of cracks and a possibility of transferring compression stress before the crack is completely closed.

In formulation of a steel constitutive law (Kojic and Bathe, 2005), we adopt the following assumptions:

steel yield occurs when strain reaches value ε_y that corresponds to stress at yield limit ε_y ,

state of failure in reinforcement occurs when the strain reaches value of limit strain ε_u ,

envelope, within which the hysteresis develops, has the "height" equal to double value of stress at yield limit (i.e. $2\sigma_y$), and

characteristics of the steel reinforcement are the same for tension and compression.

Parameters that determine the model are:

initial elasticity modulus of reinforcement E_{s0} ,

stress at yield limit σ_y ,

strain at failure limit (strength of the steel) ε_u , and

hardening modulus E_h .

In diagram of the described constitutive model the following phases are present:

state of compression or tension up to yield limit (segment of the curve 0-A),

$$\sigma_s = E_{s0} \varepsilon_s \quad \text{for} \quad \varepsilon_s \leq \varepsilon_y \quad (37)$$

yielding state (segments A-B-C or G-E-F),

$$\sigma_s = E_h \varepsilon_s \pm (\sigma_y - E_h \varepsilon_y) \quad \text{for } \varepsilon_y \leq \varepsilon_s \leq \varepsilon_u \quad (38)$$

unloading/reloading state (segment B-D-E),

$$\sigma_s = E_{so} (\varepsilon_s - \varepsilon_p) \quad (39)$$

failure state (after the point C) $\sigma_s=0$ for $\varepsilon_s \geq \varepsilon_u$.

7. Inclined cracks modeling

We adopt a smeared cracks layered model, where the inclined cracks are represented by appropriate "shifted" vertical cracks in layers. For a sufficiently large number of thin layers, the effect of inclined cracks can be achieved (schematic is shown in Fig. 9). A criterion of appearance of these "shifted" vertical cracks is the limit tension stress in concrete, caused by simultaneous action of axial and shear stresses.

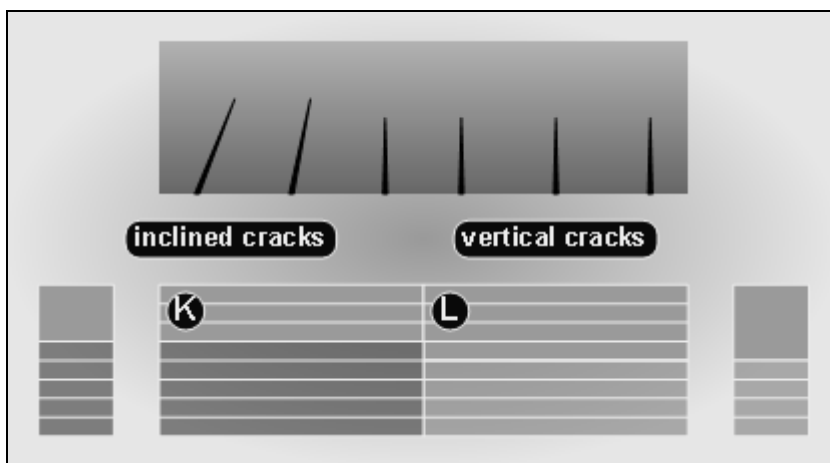


Fig. 9. Schematic of "smeared cracks approach" in inclined cracks modeling.

Relation between principal stress and, at the other side, axial and shear stress, is the classical relation:

$$\sigma_{1,2,i} = \frac{\sigma_{x,i}}{2} \pm \sqrt{\frac{\sigma_{x,i}^2}{4} + \tau_i^2} \quad (40)$$

where is: $\sigma_{1,2,i}$ are the principal stresses, $\sigma_{x,i}$ is the axial stress, and τ_i is the shear stress (all in i^{th} layer). The axial stress computation is based on the " σ - ε " concrete constitutive law, while the shear stress is computed according to the expression:

$$\tau_i = \frac{T S_i}{I b_i} \quad (41)$$

where T is the shear force, S_i is the are moment of layers above of i^{th} layer, I is the cross-section second moment, and b_i is the width of i^{th} layer.

In contrast to procedures based on design code (Fig. 10a-b), computation of " T " and " S_i " in the proposed model is performed for the entire cross-section (Fig. 10c) regardless to the stress-

strain state due to force transfer ("aggregate interlock shear transfer", "dowel action shear transfer", etc.).

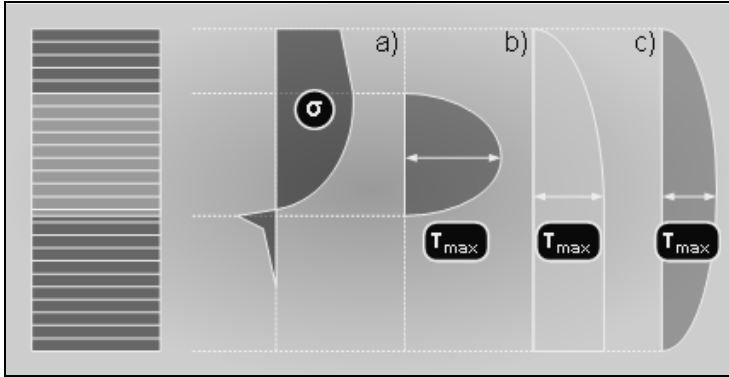


Fig. 10. Various approaches in the shear area computation.

8. Beam FE and cross-section stiffness

Layered approach makes possible to monitor the stress-strain state within the beam, as well as determination of stiffness and bearing capacity both for cross-section and for the whole beam FE. We point out several important issues in the beam discretization of a structure:

- optimum number of beam FEs for a structural system,
- optimum number of integration points within one beam FE, and
- optimum number of layers within a cross-section of the beam FE.

The error distribution indicates that the optimum number of finite elements along a beam structural element has to be, in general, between four and eight. In case of rougher division (less than 4 finite elements) contributes the analysis efficiency, but can lead to a considerable increase of the error in results. On the other hand, an increase of number of FEs along a structural beam (10 and more) does not essentially contribute to accuracy.

As mentioned above, a constant value of tangent modulus in one layer along the FE length has been adopted in our models. Namely, it can be accepted that the stiffness and bearing capacity of an element, in the section corresponding to a middle Gauss' integration point, is valid for the entire length of the finite element. This should not, in general, significantly jeopardize the solution accuracy.

In the case elastic-plastic stiffness matrix now has the following form:

$$\mathbf{k}_L = \int_A E_t dA \int_L \mathbf{B}^T \mathbf{B} dx = \sum_{i=1}^n E_t dA \int_L \mathbf{B}^T \mathbf{B} dx \quad (42)$$

The first integral reflects the characteristics of the cross-section, while the second one is a function of the beam's axial coordinate. As opposed to a standard approach, where a constant value of the modulus in one layer is assumed, we here adopt a change of tangent modulus that corresponds to constitutive law for concrete (Fig. 11).

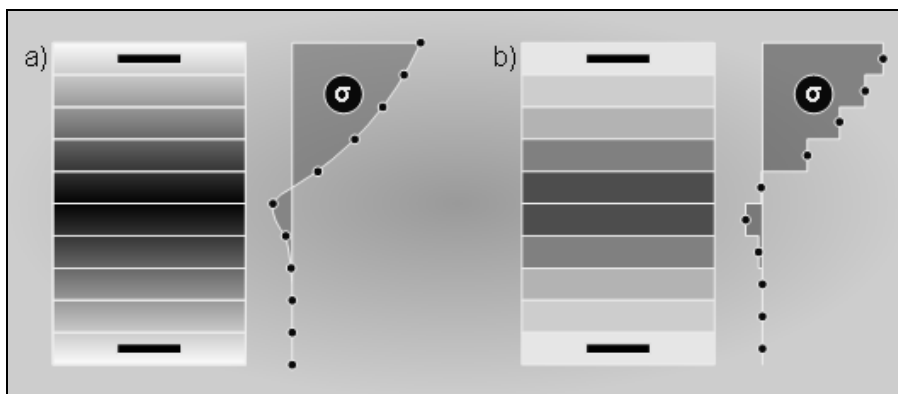


Fig. 11. Stress and tangent modulus distribution in a beam cross-section. a) Variable E_t over the beam layers; b) Constant E_t over each layer.

Adoption of continually variable stiffness along the layer height (Fig.11a) contributes to accuracy of the cross-section overall stiffness in relation to the standard approach (Fig. 11b) A force that corresponds to one layer is defined by taking the parabolic and linear distribution of stresses as follows from corresponding constitutive laws for concrete in compression and tension state.

Application of the formulated approach does not have a considerable increase of complexity and computation time. According to numerical tests given in Kovacevic (2001), a cross-section stiffness calculation, FE stiffness calculation and assembling of FE system stiffness matrix do not participate highly in the total computation time (approx. 5% for medium-scale systems and 2% for large-scale FE systems).

Based on our results, we found that the optimum layer's height is between 5% and 10% of the cross-section height. If the layers have the same thickness (what is justifiable in most cases), the optimum number of layers is between 10 and 20. By application of the standard method, with few layers (4-6), the satisfactory results can be obtained when the loading is below 50% of the limit one. In addition, small number of layers may be applied when the state of stresses is close to a uniform one (relatively large axial force of compression or tension combined with relatively small moment).

In the case of monotonous loading without unloading (what is, in fact, very rare case) with application of one-step calculation (with computing the total stresses on the basis of total strain in a layer), a small error might be obtained even without division of the cross-section into layers.

A loading with at least one cycle of unloading/reloading regime requires application of the incremental method. Then, division into a large number of layers leads to more accurate results, where the history material stress evolution is traced. Our experience is that the increase of number of layers, say over 20, does not essentially improve accuracy, and therefore a "limit" of 20 layers may be suggested.

9. Numerical tests

As an illustration of the above propositions, the results of the numerical tests are presented. We have carried out the following simple cases: one linear and two nonlinear analyses of a

simple reinforced concrete frame (Fig. 12) loaded by a seismic action. The seismic loading is selected for numerical tests because in the case of a static monotonous loading, the advantages of the proposed approach are not adequately emphasized, as is shown in Kovacevic (2006).

We next present some details about our model. The beam FE mass matrix is taken to be diagonal (lumped mass model), hence the influence of rotational inertia is neglected. The damping matrix of structure is assumed to be proportional to the initial stiffness matrix. Such an approach is used because the hysteresis dissipation effects (as consequences of material nonlinearity: appearance of cracks due to brittle concrete behavior in compressed zone, and yield of reinforcement) in nonlinear systems are dominant, as opposed to viscous damping effects present in linear systems.

For the numerical integration of dynamic equilibrium, the Newmark integration procedure (with increment $\Delta t=5ms$) is applied as well as a modified Newton-Raphson iterative procedure for balancing the residual loads. Adoption of Newmark numerical integration procedure is reasonable due to its stability and convergence, as shown in Kovacevic (2001). Modified Newton-Raphson (MNR) iterative procedure is adopted because its numerical efficiency when compared to a standard Newton-Raphson (NR) method (Bathe, 1996).

The well-known Imperial Valley (1940) seismic action, i.e. accelerogram record El Centro (Fig. 13) is used in our numerical tests.

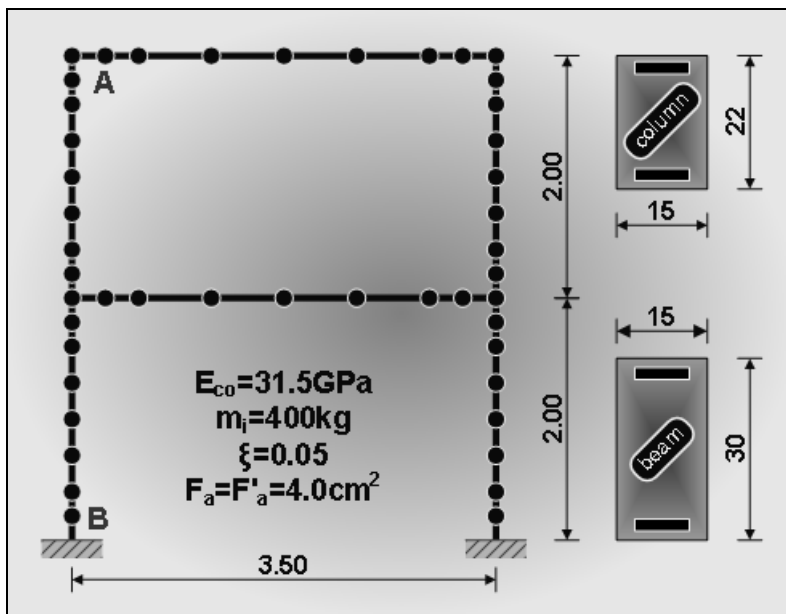


Fig. 12. Beam FE model of the RC frame used in the analysis (with initial elasticity modulus $E_{co}=31.5GPa$, concentrated mass $m_i=400kg$, coefficient of damping $\xi=0.05$ and reinforcement in tension and compression side $F_a=F'_a=4.0cm^2$).

Magnitudes, frequency configuration and form of the "main stroke" zone, made this earthquake very destructive. Differences in displacement response between "L" (linear) model and "MGS" (material-geometric nonlinear with shear effects) confirm this fact.

Besides the proportion between displacement response values, we have that in some time periods completely different behavior of RC frame model is notable, especially for this strong seismic excitation.

For the linear "L" model, maximum value of displacement is 1.855cm (for 2.5s). For nonlinear "MGS" model, the corresponding value of displacement is 2.050cm , which is about 10% larger with respect to the linear model. For time of 4.3s displacements of the linear "L" and nonlinear "MGS" model are 2.223cm and 1.776cm , respectively. Difference between displacement for "L" and "MGS" is more evident in this case – it is approximately 25%.

Due to a stiffness decrease, the "MGS" model shows a moderate reduction of frequency characteristic, which is primary considered as a prolongation of the vibration period.

Because of a comparatively small horizontal displacement and small vertical loads, for this test RC frame, the geometric nonlinearity effects are not significant. Therefore, the results of a geometric nonlinear analysis are not given to be compared.

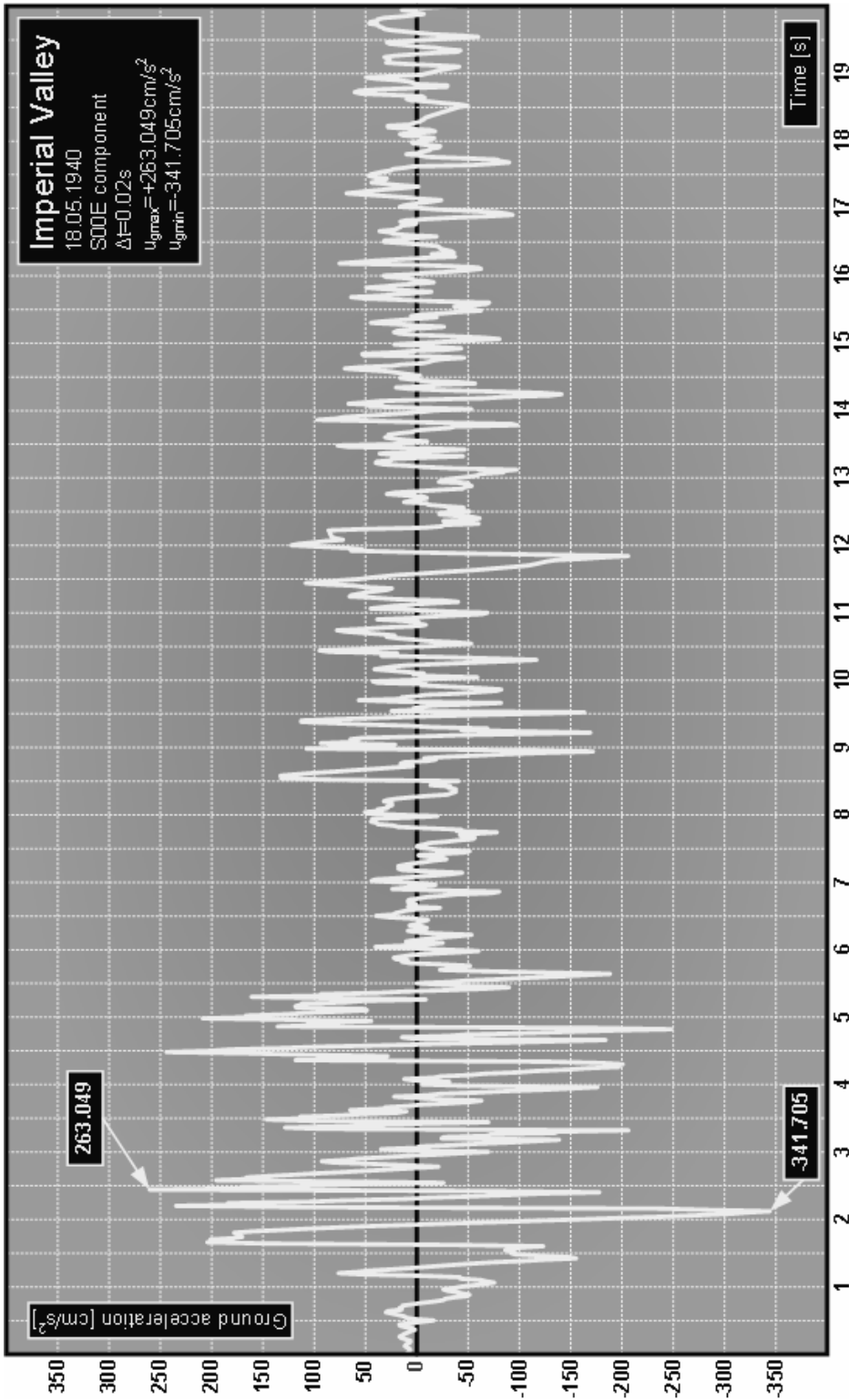


Fig. 13. Imperial Valley earthquake (El Centro accelerogram) used in the numerical test.

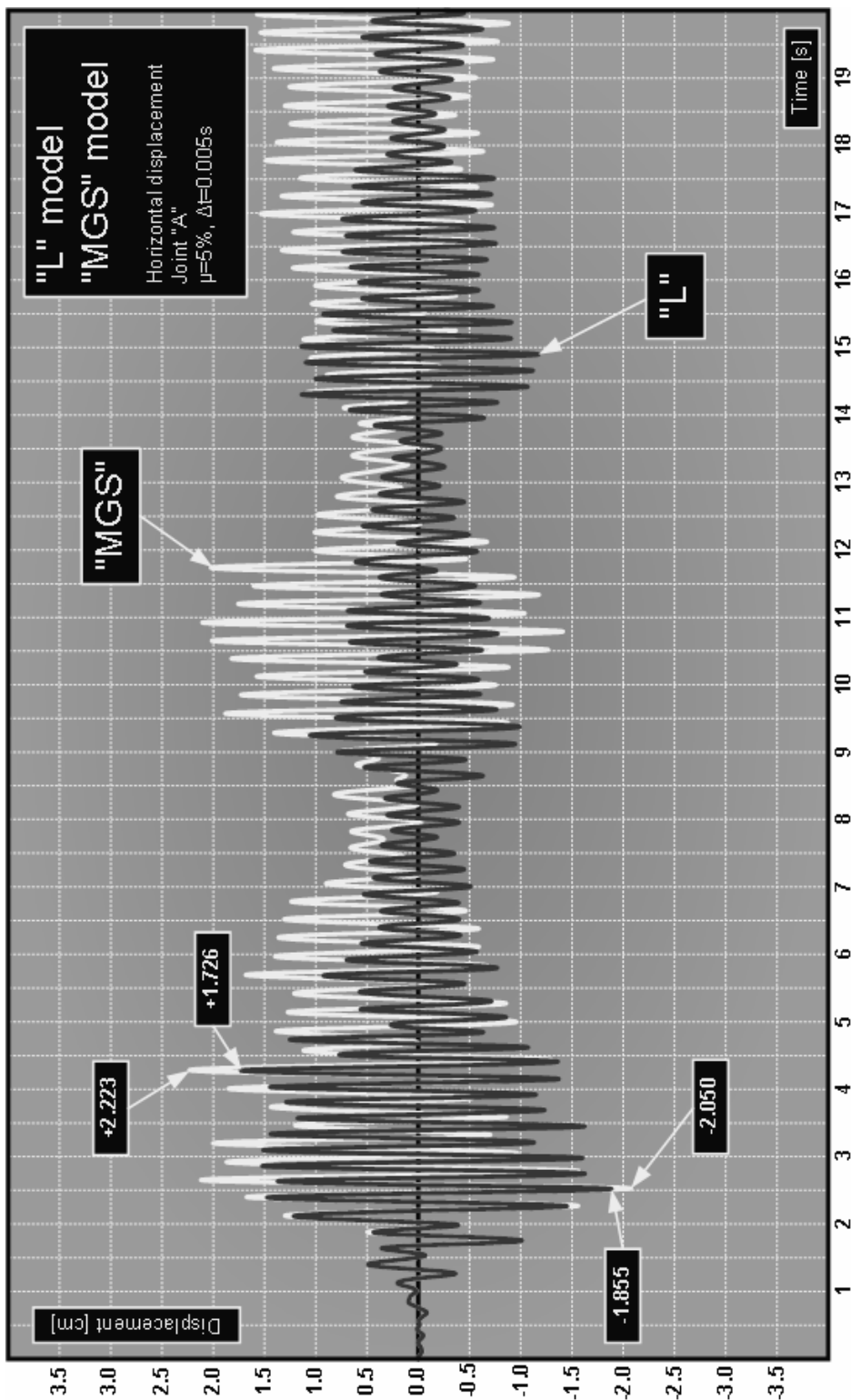


Fig. 14. Linear "L" (dark line) and nonlinear "MGS" (white line) displacement response.

9. Conclusions

The proposed numerical concept for simulation of structural behavior of RC frames loaded by seismic forces is formulated as a compromise approach. The compromise is made between the accuracy - as an essential parameter, and, on the other hand, simplicity - as the everyday design practice task. Along this line, the focus of presented report was to nonlinear analysis of the RC frame structures.

As opposed to complex 2D and 3D FE models, mostly used in theoretical considerations, a reasonably simple model is proposed. The suggested model is based on 2D beam FE with capabilities close to more sophisticated models. While in standard beam FE models only the concrete and reinforcement behavior is included, in the suggested 2D beam FE model we consider interaction of shear and flexural forces.

Verification of this modeling concept has been achieved in parametric test analyses, by comparison of the results with the experimental data and results obtained by application of complex models.

Acknowledgements This paper is a presentation of a research part in framework of the Scientific Project N^o16018 granted from Ministry of Science Republic of Serbia

References

- Bathe KJ (1996) Finite Element Procedures, Prentice-Hall, Englewood-Cliffs, USA.
- Blaauwendraad J & De Groot AK(1983). Progress in Research on Reinforced Concrete Plane Frames, HERON, Vol. 28, No. 2, Delft.
- Burns NH & Siess CP (1966). Repeated and Reversed Loading in Reinforced Concrete, Journal of the Structural Division, ASCE, Vol. 92, No. 5, New York, 65-78.
- CEB Bulletin d'information No 210 (1991) Behavior and Analysis of Reinforced Concrete Structures under Alternate Actions Inducing Inelastic Response, Vol. 1: General Models, Lausanne.
- Kojic M and Bathe KJ (2005). Inelastic Analysis of Solids and Structures, Springer-Verlag, Berlin-Heidelberg, 2005.
- Kovačević D (2001). Numerical modeling of Behavior of Reinforced Concrete Frames Loaded by Seismic Actions (in Serbian), Ph.D. Thesis, Civil Engineering Faculty, University of Belgrade, 185.
- Kovačević D (2006): FEM Modeling in Structural Analysis. (in Serbian), Građevinska knjiga, Belgrade, 336.
- Sekulović M, Milašinović D and Kovačević D (1996). Increasing of Numerical Efficiency in Nonlinear Analysis of Reinforced Concrete Beam Elements, CST '96 - 3rd International Conference on Computational Structures Technology, Ed. B.H.V. Topping, Civil-Comp. Press, Meigle Printers, Scotland, 139-150.
- Semi-rigid Structural Connections (1996), IABSE Colloquium Report, Istanbul.
- Scordelis A (1984). Computers Models for Nonlinear Analysis of Reinforced and Prestressed Concrete Structures, PCI Journal, No 11-12, 116-135.